

# Non-Equilibrium Reaction Rates in Hydrogen Combustion

Stephen J. Voelkel<sup>1</sup>, Venkat Raman<sup>2</sup>, Philip Varghese<sup>1</sup>

<sup>1</sup>The University of Texas at Austin, Austin, TX 78712, USA

<sup>2</sup>The University of Michigan, Ann Arbor, MI, 48109, USA

## 1 Introduction

Vibrational non-equilibrium in hydrogen-air mixtures plays an important role in reactive high speed conditions. Specifically, non-equilibrium occurs near post shock interfaces and the gas mixture relaxes back to equilibrium downstream. This relaxation timescale is non-negligible, and as a result, models that include non-equilibrium effects for these systems are required. Many current models introduce a reaction mechanism based on multiple temperatures [1] [2]. For instance, a common two-temperature model associates the the molecular translational and rotational energy distributions with a single temperature  $T$ , and the molecular vibrational energy distribution with another temperature  $T_v$ . The current proposal is to expand these models to include species-specific vibrational distributions. Specifically, rather than a single vibrational temperature for the entire set of species, each species will have its own vibrational temperature. Developing this new model requires non-averaged, state-specific reaction rates, which are to be calculated using a quasi-classical trajectory (QCT) technique. Additionally, the calculated overall reaction rates based on state-specific rates are fundamentally based rather than being purely *ad hoc*. The calculation of these state-specific reaction rates and the resulting modified chemical mechanism are the focus of the current work.

## 2 State-specific Reaction Rates

For a given reaction, the initial internal state of the reactants is defined by a set of vibrational and rotational quantum numbers, denoted  $\mathbf{v}$  and  $\mathbf{J}$ , respectively. Likewise, the products have a final internal state, denoted  $\mathbf{v}'$  and  $\mathbf{J}'$ . In a QCT framework,  $\mathbf{v}$  and  $\mathbf{J}$  restrict the space of allowable orientations and motions of each molecule, which is then sampled from to initiate trajectories. The relative velocity of the reactant molecules is sampled assuming the translational energy can be characterized by a single temperature  $T$  (*i.e.* the system is in translational equilibrium). Once the initial conditions are known, the dynamics of the nuclei follow a deterministic path from classical mechanics where the driving force is defined by the potential energy surface (PES), which is calculated by quantum chemistry methods.

The state-specific probability of the reaction  $P_r$  is the fraction of trajectories with appropriately sampled initial conditions that result in the desired products. In this formulation,  $P_r$  is dependent on the internal states of the reactants and products, the relative speed  $g$ , and the impact parameter  $b$ . The number

of required trajectories is dependent on the rate of convergence of  $P_r$  to a fixed value. Once  $P_r$  is determined, the state-specific reaction cross-section is

$$\sigma(\mathbf{v}, \mathbf{J}, \mathbf{v}', \mathbf{J}', g) = \int_0^\infty 2\pi b P(\mathbf{v}, \mathbf{J}, \mathbf{v}', \mathbf{J}', g, b) db. \quad (1)$$

For a system in thermal equilibrium, the relative speed is integrated over its range and weighted by the Maxwell speed distribution,  $\chi_M(g; T)$ . The result is the state-specific reaction rate given by

$$k(\mathbf{v}, \mathbf{J}, \mathbf{v}', \mathbf{J}'; T) = \int_0^\infty g \chi_M(g; T) \sigma(\mathbf{v}, \mathbf{J}, \mathbf{v}', \mathbf{J}', g) dg. \quad (2)$$

Multi-temperature models, such as the two-temperature model addressed in Section 1, assume that each energy mode follows a Boltzmann distribution characterized by a temperature unique to that specific mode. If the state-specific reaction rates from Eq. (2) are known, the multi-temperature rates are defined by averaging said rate over the appropriate distributions of the reactant states. For example, if the rotational and vibrational energy distributions can be characterized by Boltzmann distributions dependent on the macroscopic temperatures  $T_r$  and  $T_v$ , respectively, then the three-temperature reaction rate becomes

$$k(T, T_r, T_v) = \sum_{\mathbf{J}} f_r(\mathbf{J}; T_r) \sum_{\mathbf{v}} f_v(\mathbf{v}; T_v) \left( \sum_{\mathbf{J}'} \sum_{\mathbf{v}'} k(\mathbf{v}, \mathbf{J}, \mathbf{v}', \mathbf{J}'; T) \right), \quad (3)$$

where the product states are summed over, and  $f_v$  and  $f_r$  are the vibrational and rotational Boltzmann energy distributions of the reactants. It is important to note that the decoupling of rotation and vibration energy distributions is a further approximation, so this limitation must be accounted for.

The rotational temperature relaxes relatively quickly to the translation temperature when compared to the relaxation of the vibrational temperature and other physical phenomena (reaction and mixing timescales), so the rotational Boltzmann distribution is sufficiently characterized by the translational temperature, or  $T_r = T$  in Eq. 3. The proposed reaction rate model makes use of this assumption, but it expands the vibrational state information by defining a set of vibrational temperature  $\mathbf{T}_v = \{T_{v,1}, T_{v,2}, \dots, T_{v,N_r}\}$  for  $N_r$  reactants. The final result modifies Eq. 3 so that

$$k(T, \mathbf{T}_v) = \sum_{\mathbf{J}} f_r(\mathbf{J}; T) \sum_{\mathbf{v}} f_v(\mathbf{v}; \mathbf{T}_v) \left( \sum_{\mathbf{J}'} \sum_{\mathbf{v}'} k(\mathbf{v}, \mathbf{J}, \mathbf{v}', \mathbf{J}'; T) \right). \quad (4)$$

The chemistry model must account for energy exchange between the translational and multiple vibrational modes and also for vibrational energy exchange between the species.

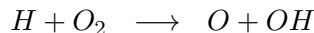
### 3 Calculation of State-Specific Cross-Sections

As previously mentioned, the state-specific cross-sections and subsequent reaction rates are calculated using a QCT methodology adapted from the VENUS program [3]. Retaining state-specific information restricts us from selectively sampling the initial conditions, which in general washes out this level of detail. Instead, to retain state-specific information, each state-specific reaction cross-section is independently calculated based on trajectories sampled from the full space of initial conditions. That is, a new set of trajectories parametrized by a specific reactant internal state, product internal state, and reactant relative speed are simulated for each cross-section.

Once the cross-sections are calculated, they are archived as a library. The cross-sections are then recalled to define specific reaction rates. Because the cross-sections are state-specific, many different types of averaging or state-specific reaction rates can be studied.

## 4 Results and Observations

As a first step in studying hydrogen combustion, the chain-branching reaction



has been studied using the new QCT framework for large scale simulations and tabulation. The PES used for these preliminary calculations was previously developed by Melius and Blint [4]. This surface was chosen for simplicity and speed of calculation, but more detailed PESs will be utilized in future calculations. The impact parameter for each initial state sampled 20 impact parameters from 0 Å to 5 Å and then ran 20 trajectories for each impact parameter. To allow for averaging over a large range of translational temperatures, 158 relative speeds were sampled. Finally, 2,399 internal states of  $O_2$  were sampled. For the preliminary calculations, the cross-sections were only averaged, so the final internal states were not stored. In summary, 379,042 cross-sections were calculated, and 151,616,800 trajectories were simulated. On the Lonestar cluster of the Texas Advanced Computing Center (TACC), the job was run on 2,040 cores for approximately 10 hours.

We initially studied the efficiency function  $\varphi$  of the non-equilibrium rate [2]; specifically

$$\varphi = \frac{k(T, T_v)}{k(T, T_v = T)}, \quad (5)$$

where the reaction rate is calculated by Eq. 4 where  $T_v$  is the vibrational temperature of  $O_2$ . The logarithm of the efficiency function for  $T$  and  $T_v$  ranging from 500 K to 20,000 K is shown in Figure 1. Along the diagonal the efficiency is unity, for  $T_v > T$  the efficiency is increased, and for  $T_v < T$  the

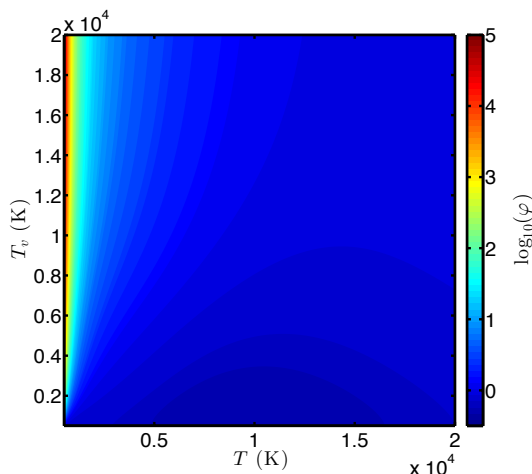


Figure 1: Efficiency function contours based on state-specific QCT calculations.

efficiency is decreased. Diagonal slices along the contour plot for specific  $T - T_v$  differences are shown in Figure 2. The figure shows that in general,  $T_v > T$  has a greater impact on the efficiency relative to  $T_v < T$ . For temperatures of 2,000 K and higher, the efficiency approaches unity for moderate differences between  $T$  and  $T_v$ . Specifically, for  $T > 2,500$  K and  $T_v = T \pm 500$  K, the non-equilibrium rate is within approximately 13% of the equilibrium rate. For  $T > 10,000$  K, this drops to within approximately 3% of the equilibrium rate. For temperatures below 2,000 K, the non-equilibrium effects become more pronounced. For  $T_v = T + 500$  K, the non-equilibrium rate increases by approximately 13% at 2,500 K and 75% at 1,000 K. For  $T_v < T$ , the effect is less dramatic. For  $T_v = T - 500$  K, the

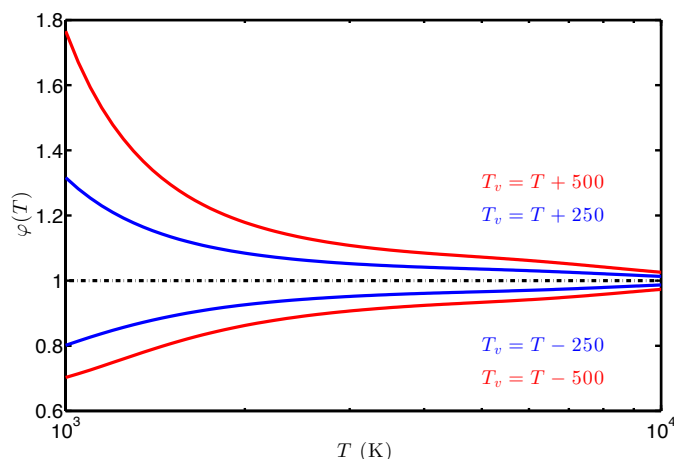


Figure 2: Efficiency function for specific  $T - T_v$  differences based on state-specific QCT calculations.

non-equilibrium rate decreases by approximately 11% at 2,500 K and 30% at 1,000 K. Other moderate temperature differences show similar results, as seen for  $T_v = T \pm 250$  K in Figure 2.

The QCT calculations are checked by calculating the thermally averaged equilibrium rate from the cross-sections, denoted by  $k_{eq}(T) = k(T, T_v = T)$ . The results in Figure 3 show reasonable agreement with a recent shock tube study's best fit rate [5], which is valid for 1,100-3,370 K. Excellent agreement

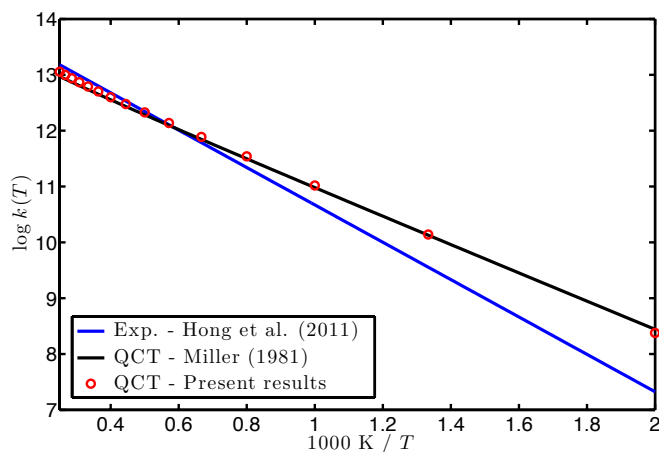


Figure 3: Thermally averaged reaction rate,  $k_{eq}(T)$ , from this study and from studies by Hong et al. [5] and by Miller [6].

is observed when compared to Miller's QCT-derived rate using the same PES [6], which is valid for 250-2,500 K.

The current non-equilibrium rates are also compared with Park's two-temperature model [1] in which the non-equilibrium rate is equal to the equilibrium rate at a modified temperature dependent on  $T$  and  $T_v$ . Specifically,

$$k_{Park}(T, T_v) = k_{eq}(\sqrt{TT_v}). \quad (6)$$

Figure 4 shows Park's model normalized by the non-equilibrium rate from Figure 1, denoted by  $k_{neq}$ . In

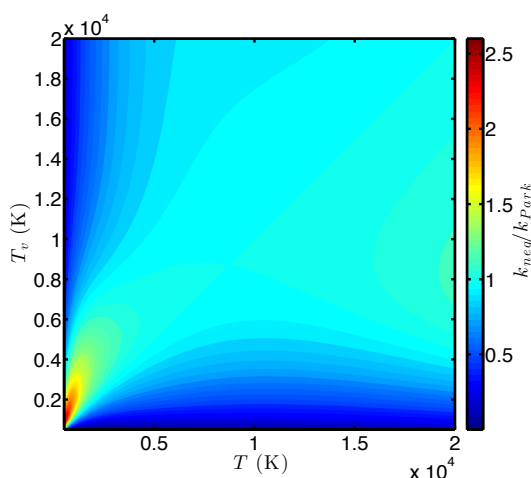


Figure 4: Non-equilibrium reaction rate calculated from Park's model normalized by the non-equilibrium rate from this study.

general, for temperatures above 5,000 K and  $T_v$  within 1,000 K of  $T$ , Park's model performs adequately. However, for temperatures in the range from 500 to 5,000 K, small deviations of the vibrational temperature from the translational temperature result in significant discrepancies compared to the present calculations. Specifically, for  $T_v < T$ , the non-equilibrium rate of Park's model is significantly lower than the current results. For  $T_v > T$ , the non-equilibrium rate of Park's model is higher than the current results (the dark red region of Figure 4). Figure 5 shows slices of the efficiency function at  $T_v = T \pm 250$  for Park's model and the present results in Figure 2. For  $T_v = T + 250$  K, the Park's model increases

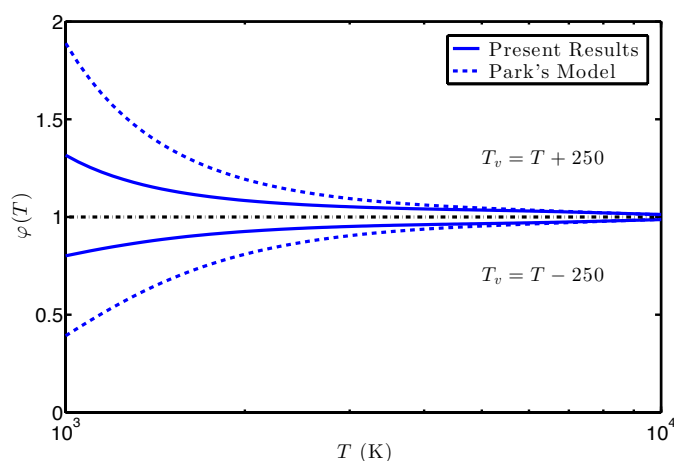


Figure 5: Efficiency function for specific  $T - T_v$  differences based on Park's model and state-specific QCT calculations.

the efficiency by approximately 7% at  $T = 2,500$  K and 57% at  $T = 1,000$  K. For  $T_v = T - 250$  K, the Park's model decreases the efficiency by approximately 7% at  $T = 2,500$  K and 41% at  $T = 1,000$  K. In summary, for the reaction  $H + O_2 \rightarrow O + OH$ , Park's two-temperature model is too sensitive

regarding  $T - T_v$  differences, so it overestimates the effect of thermodynamic non-equilibrium has on the reaction.

## 5 Conclusion

A non-equilibrium reaction rate model for hydrogen-air combustion that utilizes a vibrational temperature for each chemical species has been presented. This model requires state-specific cross-sections of each reaction in the hydrogen-air reaction mechanism. State-specific cross-sections of the chain branching reaction  $H + O_2 \rightarrow O + OH$  were calculated by a QCT technique. The subsequent non-equilibrium reaction rates were attained by averaging the cross-sections over Boltzmann distributions dependent on the translational temperature and the vibrational temperature of  $O_2$ . These rates were compared to Park's two-temperature model, which showed that Park's model overestimates the effect of thermodynamic non-equilibrium or temperature below 5,000 K.

## References

- [1] C. Park (1994). Review of chemical-kinetic problems of future NASA missions. I - Earth entries. *J. Thermophys. Heat Transfer* 7:385-398.
- [2] O. Knab, H.-H. Fruhauf, E.W. Messerschmid (1995). Theory and validation of the physically consistent coupled vibration-chemistry-vibration model. *J. Thermophys. Heat Transfer* 9: 219-226.
- [3] W.L. Hase, R.J. Duchovic, X. Hu, A. Komornicki, K.F. Lim, D.-H. Lu, G.H. Peslherbe, K.N. Swamy, S.R.V. Linde, A. Varandas, H. Wang, and R.J. Wolf (1996). *Quantum Chem. Program Exchange* 16: 671.
- [4] C.F. Melius, R.J. Blint (1979). Potential energy surface of the  $HO_2$  molecular system. *Chem. Phys. Lett.* 64: 183.
- [5] Z. Hong, D.F. Davidson, E.A. Barbour, R.K. Hanson (2011). A new shock tube study of the  $H + O_2 \rightarrow OH + O$  reaction rate using tunable diode laser absorption of  $H_2O$  near  $2.5 \mu\text{m}$ . *Proc. Combust. Inst.* 33: 309-316.
- [6] J.A. Miller (1981). Collision dynamics and the thermal rate coefficient for the reaction  $H + O_2 \rightarrow OH + O$ . *J. Chem. Phys.* 74: 5120.